Chemical Physics Letters 539–540 (2012) 151–156

Contents lists available at SciVerse ScienceDirect

Chemical Physics Letters

journal homepage: www.elsevier.com/locate/cplett

Study of the reactive excited-state dynamics of delipidated bacteriorhodopsin upon surfactant treatments

Chi-Wen Cheng [a], Yuan-Pern Lee [a,b,*], Li-Kang Chu [c,*]

[a] Department of Applied Chemistry and Institute of Molecular Science, National Chiao Tung University, 1001 Ta-Hsueh Rd., Hsinchu 30013, Taiwan
[b] Institute of Atomic and Molecular Sciences, Academia Sinica, Taipei 10617, Taiwan
[c] Department of Chemistry, National Tsing Hua University, 101, Sec. 2, Kuang-Fu Rd., Hsinchu 30013, Taiwan

ARTICLE INFO

Article history:
Received 12 March 2012
In final form 3 May 2012
Available online 10 May 2012

ABSTRACT

The dynamics of the reactive excited-state of bacteriorhodopsin treated with various surfactants have been investigated through the measurement of pump–probe absorption spectra. Upon excitation of bR at 570 nm in the presence of ionic surfactants CTAB and SDS, the lifetime of the reactive excited-state of the all-*trans* protonated Schiff base, probed at 460 nm, was observed to increase up to 20%, whereas an insignificant change was observed upon addition of neutral surfactant C6E2. Measurements of steady-state absorption spectra, fluorescence, and circular dichroism indicated that the bR suspensions retain their trimeric configuration with partial delipidation. This removal of lipids causes a structural alteration and the varied excited-state dynamics.

1. Introduction

Bacteriorhodopsin (bR) is a natural photosynthetic protein in which the bR unit is composed of seven α-helices and an interior retinal that is covalently linked to Lys216 [1]. The trimeric units of bR surrounded by lipids (25% by mass), known as the purple membrane, are a part of the membrane of *Halobacterium halobium* [2]. The absorption of yellow light initiates the isomerization of the interior retinal chromophore from the all-*trans* to the 13-*cis* form, followed by spectrally distinguishable intermediates in a sequence, and results in a net proton transport from the cytoplasm to the extracellular phase [3].

Extensive ultrafast measurements of the primary step of the bR photocycle, involving a vertical transition along the C_{13}=C_{14} isomerization coordinate, have been reported [4–14]. The reactive excited state of lifetime ~500 fs, denoted as intermediate I [4–10], is characterized with maximum absorption at ~460 nm followed by a relaxation to generate the 13-*cis* configuration [11–14].

The excited-state dynamics has been investigated with numerous quantum-chemical simulations at high levels [15–20]. Tachikawa and Iyama performed time-dependent DFT calculations to predict the dependence of the energy on the reaction coordinate of dihedral angle Q_{13-14} along the C_{13}=C_{14} bond, and obtained a barrier of height 52 kJ mol^{-1} at Q_{13-14} = 58° with respect to the energy well of the S_1 state; this barrier results from an avoided crossing between S_1 (B_u-like) and S_2 (A_g-like) excited states [18]. Cembran et al. employed a multiconfigurational perturbation method, CASPT2//CASSCF, to account for the effects of the orientation of the counterion on the isomerization potential-energy curve in terms of an electrostatic interaction of the counterion with the retinal; they concluded that relocation of the negative charge of the deprotonated amino acids near the C_{13}=C_{14} bond is capable of altering the height of the exit barrier toward the conical intersection [16]. Altoè et al. used a model involving an asynchronous bicycle-pedal deformation of the C_{10}=C_{11}–C_{12}=C_{13}–C_{14}=N moiety to describe the retinal isomerization and derived a barrier <1 kJ mol^{-1} for the relaxation of intermediate I [20].

In addition to investigations on the native trimeric bR, several chemical and physical treatments were introduced to perturb the retinal isomerization dynamics [21–23]. Increasing the pH to an alkaline condition results in a substantial increase in the lifetime of intermediate I, from 0.46 to >1.1 ps with nearly the same quantum yield [21]. The reestablished equilibrium of the acid–base pairs in the vicinity of the retinal results in a variation of the electronic and steric factors in the retinal isomerization. Zgrablić et al. examined the effect of protic solvents on the dynamics of retinal isomerization, and demonstrated that the ultrafast dynamics are dominated by intramolecular processes, likely due to mild structural changes near the retinal [22]. Apart from chemical treatments, Biesso et al. employed an optically induced plasmonic field via photoexcitation of gold nanoparticles on the retinal isomerization and found that the lifetime of intermediate I was increased to 800 fs [23].

* Corresponding authors. Addresses: Department of Applied Chemistry and Institute of Molecular Science, National Chiao Tung University, 1001 Ta-Hsueh Rd., Hsinchu 30010, Taiwan (Y.-P. Lee), Department of Chemistry, National Tsing Hua University, 101, Sec. 2, Kuang-Fu Rd., Hsinchu 30013, Taiwan (L.-K. Chu).
E-mail addresses: yplee@mail.nctu.edu.tw (Y.-P. Lee), lkchu@mx.nthu.edu.tw (L.-K. Chu).

0009-2614/$ - see front matter © 2012 Elsevier B.V. All rights reserved.
http://dx.doi.org/10.1016/j.cplett.2012.05.006

To complement the analysis of properties of the native bR, monomerized bR and site-specifically mutated bR were also investigated [24,25]. Song et al. replaced charged amino acids of the protein near the retinal with neutral ones and observed a decreased rate of isomerization by factors 4–20; they concluded that the ground and excited states are strongly perturbed through an electrostatic interaction between the retinal and the protein moiety [24]. Using the neutral surfactant Triton X-100 to monomerize bR suspensions, Wang et al. observed an increased lifetime of intermediate I [25]; they attributed the altered kinetics of the retinal isomerization to subtle variations of the charge distribution in the protein interior and the uncoupling of the dipole interactions between each retinal in the trimeric bR unit.

In this work, we added neutral (diethylene glycol mono-*n*-hexyl ether, C6E2), cationic (cetrimonium bromide, CTAB), and anionic (sodium dodecyl sulfate, SDS) surfactants to bR suspensions to perturb the kinetics of intermediate I, monitored at 460 nm. The kinetics of the M and O intermediates have been proved to be perturbed in the presence of surfactants [26,27]. Our observed temporal behaviors showed significant variations and are discussed in terms of the coupling of retinal and neighboring amino acids when the structure alters upon removal of the native lipids with surfactants.

2. Materials and methods

2.1. Sample preparation

The native bR from the purple membrane of *Halobacterium salinarium* was prepared according to a standard method [28]. After purification and photoactivation via irradiation with a Xe lamp for 1 h, UV–Vis spectra of the steady-state light-adapted bR were collected to confirm the purity. The concentrations of the bR suspensions were determined using absorption coefficient $\varepsilon_{568} = 62{,}700\ M^{-1}\ cm^{-1}$ for the light-adapted state [29].

The bR suspensions were dispensed into micro-centrifuge tubes and stored at −10 °C for further use. Three surfactants, CTAB (Sigma, 99%), SDS (Sigma, 95%), and C6E2 (TCI America, 95%), and buffer solution (pH = 7.1, phosphate) were diluted for subsequent mixing with bR. The samples were prepared on mixing fixed amounts of bR with varied amounts of the dilute surfactants in a buffer solution. The final concentrations of the buffer solution and the bR suspension were controlled at 1.25 mM and 21 μM, respectively in each sample. The mixtures were irradiated with white light to obtain the light-adapted bR. The pH conditions were controlled within ±0.1 unit.

2.2. Steady-state spectra

Ultraviolet–visible (UV–Vis) absorption spectra in the steady state were recorded with a spectrometer (Varian, Cary 50) before and after the pump–probe experiments. The circular dichroism (CD) spectra were also recorded (AVIV spectrometer, model 410, spectral resolution 1 nm). The CD signals were averaged for 20 s at each wavelength; all measurements were made at 25 °C. Cuvettes with optical paths of lengths 0.2 and 1 cm were employed in these measurements, respectively. The fluorescence of the steady state at 25 °C was measured with a spectrophotometer (Hitachi, F-7000) using a quartz cuvette with an optical path of 1 cm. With excitation at 280 nm, the emission was recorded from 300 to 500 nm with scanning step 1 nm.

2.3. Femtosecond pump–probe spectra

The femtosecond transient absorption was recorded with a conventional pump–probe method [30]. The laser pulses were amplified with a regenerative amplifier (Legend-USP-1K-He, Coherent) seeded with a mode-locked Ti:sapphire laser system (Mantis-Seed/Verdi V5, Coherent) and pumped with a Nd:YLF laser (Evolution 30, Coherent, 1 kHz). The generated pulses of duration ~40 fs were centered at 800 nm with average energy 2.5 mJ $pulse^{-1}$. The output pulse at 800 nm was split into two parts to generate the pump and probe beams; one part was directed into an optical parametric amplifier (OPerA-F, Coherent) to generate the near-IR pulses at 1.84 μm, followed by fourth-harmonic generation (FHG) of the idler wave to generate the probe beam at 460 nm. The other part of the pulse served to generate a pump beam at 570 nm by sum-frequency generation (SFG) of another OPA output at 1.95 μm with 800 nm. The probe was separated into two parts for use as sample and reference pulses and detected with two Si photodiodes. The optical delay between the pump and probe beams was controlled with a stepping translational stage. Every alternate pump pulse was blocked with a synchronized chopper at 500 Hz; the absorbance change (ΔA) was calculated from sequential pump versus un-pumped probe pulses. The energies of the pump pulses were appropriately attenuated to 60 nJ to avoid degradation of the bR sample. The sample cell was rotated so that each pump pulse excited a fresh bR sample.

3. Results and discussions

Steady-state absorption, fluorescence and circular dichroism spectra were recorded to identify the configuration of the bR suspensions upon the treatment with surfactants. The corresponding kinetics of intermediate I were investigated with an ultrafast pump–probe technique.

3.1. Steady-state UV–Vis absorption

The absorption spectrum of the light-adapted bR, shown in the black trace of Figure 1A, is characterized by three bands in the ultraviolet and visible spectral regions [31]. The intense band with its maximum at 568 nm ($\varepsilon_{568} = 62{,}700\ M^{-1}\ cm^{-1}$) and the broad band extending from 300 to 450 nm without a prominent maximum are attributed to absorption by the retinal chromophore. The intense absorption with a maximum near 280 nm is attributed mainly to the tryptophan and tyrosine residues, but also in part to the retinal chromophore.

The steady-state UV–Vis absorption spectra of bR upon surfactant treatment are shown in Figure 1A. A comparison of the absorbance and corresponding maxima of the untreated and surfactant-treated bR reveals that neutral surfactant C6E2 distorts the absorption contour insignificantly, but the anionic surfactant SDS, in particular, decreased the absorbance of the retinal and the tryptophan residues. The addition of the cationic surfactant CTAB did not obviously bleach the retinal absorbance, but increased the absorbance below 500 nm. The inset in Figure 1A represents the absorption contours normalized with respect to the intensity maximum of the retinal moiety at 568 nm. The normalized absorbance of retinal in the range 700–460 nm doubled. This baseline drift has been proposed to be due to scattering as measuring the absorption coefficient of the bR suspensions [31]. On adding further CTAB, the baseline was effectively raised because of the formation of micelles of CTAB that lead to effective scattering, but the micelles did not deplete bR severely so that no fatal alteration was observed in the circular dichroism and fluorescence measurements as shown in Section 3.2. and 3.3.

Wang et al. reported that the absorption contour of monomeric bR shifts hypsochromically to a maximum at 553 nm [25]. The absorption contour of the retinal in 75% delipidated bR exhibits a blue shift 10 nm [32]. Figure 1B relates the absorption maxima to

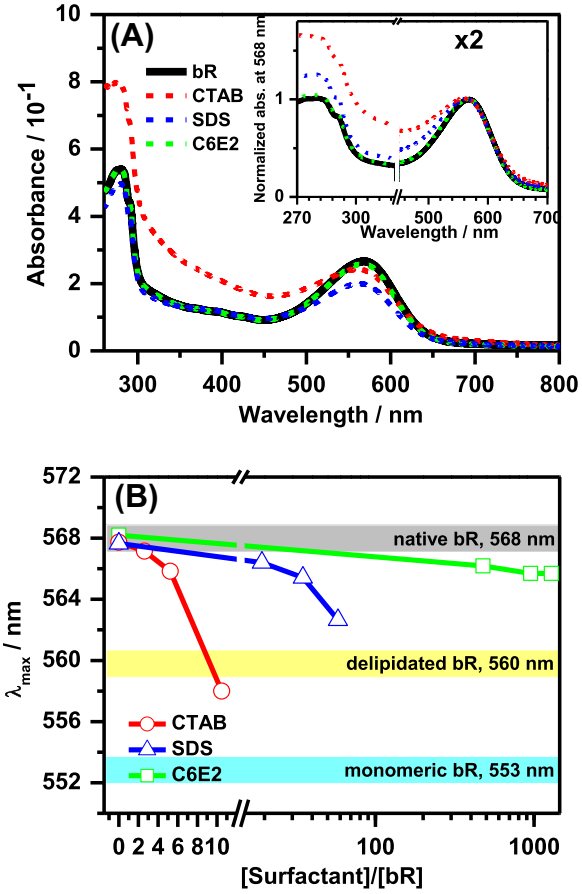

Figure 1. (A) Absorption spectra of bR upon surfactant treatment; the inset presents absorption contours normalized with respect to the absorption maximum of the retinal moiety at 568 nm. The concentrations are [bR] = 21 μM, [buffer solution] = 1.25 mM, [CTAB] = 0.22 mM, [SDS] = 1.22 mM, and [C6E2] = 27 mM. (B) λ_{max} of absorption of the retinal moiety versus concentration of surfactant. The gray, yellow and blue columns represent λ_{max} of the absorption for native, delipidated and monomeric bR, respectively.

the surfactant concentrations. Upon gradual addition of the surfactant CTAB, the shift of the absorption maximum approaching 560 nm indicates that the bR suspensions become delipidated, but retain the trimeric configuration that is confirmed with circular dichroism spectra in Section 3.3. Previous authors showed that further addition of CTAB partially monomerized the bR suspension, as indicated by a shift of the absorption maximum to 553 nm and a decreased absorbance in the range 450–300 nm because of the decreased volume of the monomerized bR. A similar trend toward delipidated bR was observed on the treatment with SDS, but was insignificant for C6E2. As a result, ionic surfactants CTAB and SDS are more effective than the neutral C6E2 in removing the lipids from the bR suspensions.

3.2. Steady-state fluorescence spectra

Steady-state fluorescence spectra provide information on the chemical environment around the bR suspensions in terms of the emission contours of the constituent tryptophans [33]. The bR monomeric unit contains two amino acids with aromatic rings, tryptophan and tyrosine, in a molar ratio 8:11 [34]. Upon photoexcitation at 280 nm, the fluorescence of the tryptophan is observed about 330 nm [35]. Reshetnyak et al. demonstrated that the emission contour at 307–355 nm upon excitation of the tryptophan moiety in a protein can be characterized according to an interaction between the tryptophan and adjacent amino acids and water

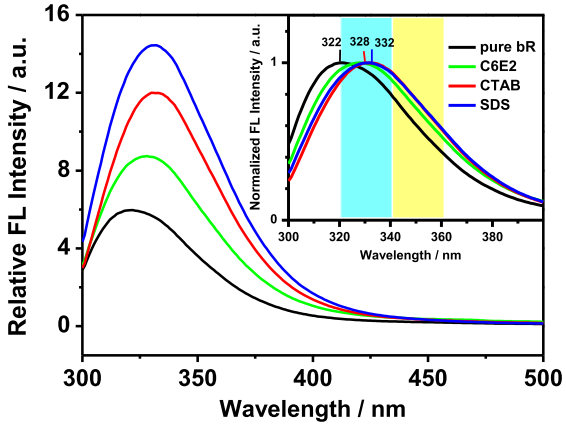

Figure 2. Fluorescence spectra upon excitation of bR at 280 nm in the presence of surfactants. The concentrations are [bR] = 21 μM, [buffer solution] = 1.25 mM, [CTAB] = 0.22 mM, [SDS] = 1.22 mM and [C6E2] = 27 mM. The normalized contours are shown in the inset. The blue and yellow columns represent the emission maximum of the tryptophan in dehydrated and aqueous environments, respectively.

[36]. Schenkl et al. indicated that Trp86, Trp182, Trp138 and Trp189 exhibit a notable interaction with retinal [37]; the corresponding emissions of these exciplexes are characterized at 316–331 nm [36]. Trp10 and Trp12 are located at the boundary of the extracellular side in contact with bound water and can be characterized at 340–353 nm [36]. Trp137 and Trp80 did not exhibit a strong interaction with retinal and adjacent residues; they can be treated as isolated tryptophans emitting at 308 nm [36]. Moreover, Plotkin and Sherman demonstrated that the hydrated environment near the tryptophan residues produces a bathochromic emission of the fluorescence spectra [38]. The steady-state fluorescence spectra of the tryptophan moiety upon excitation of bR at 280 nm are shown in Figure 2, with normalized contours in the inset. The addition of a surfactant results in enhanced fluorescent intensity with a bathochromic emission shift toward 350 nm. The delipidation induces a conformational change that leads to the decoupling between the tryptophans and retinal. As a result, the population of the excited state of tryptophan upon excitation at 280 nm does not become degraded via energy transfer from tryptophan to retinal, and results in increased fluorescent intensity. This red-shifted contour reveals that the original lipid-surrounded bR suspensions become delipidated, thus exposing bR to an aqueous environment; Trp10 and Trp12 might be responsible for the bathochromic shift. Ionic surfactants CTAB and SDS are consequently more effective than the neutral C6E2 in removing the circumjacent lipids from the proteins. This conclusion is consistent with the UV–Vis absorption spectra in the steady state.

3.3. Circular dichroism spectra

Visible circular dichroism (CD) spectra were employed to examine the existence of the trimeric configuration of the bR according to the characteristic biphasic ellipticity, which exhibits a positive lobe at small wavelengths and a negative lobe of equal ellipticity at large wavelengths with a crossing at 574 nm [39]. The magnitude of the molar ellipticity indicates the strength of the coupling of the retinals in the trimeric bR, which is inversely proportional to the cube of the distance of the dipolar interaction [40]. When the trimeric bR becomes monomerized (or isolated), the decoupling of the excitons produces a monophasic contour with a maximum at 550 nm [39]. Both biphasic and monophasic contours vanish when the bR becomes denatured.

The CD measurements of bR upon surfactant treatments are shown in Figure 3. The addition of the neutral surfactant affected

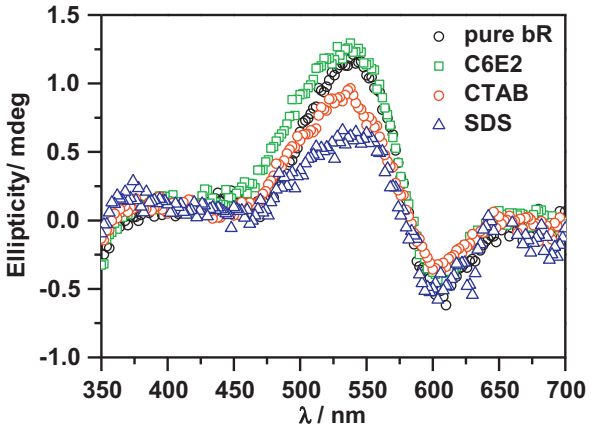

Figure 3. Circular dichroism spectra of light-adapted bR (21 μM) in CTAB (0.22 mM), SDS (1.22 mM), and C6E2 (27 mM) in phosphate buffer solutions (1.25 mM).

the CD contour insignificantly relative to the native bR, but the addition of the ionic surfactants decreased the magnitude of the molar ellipticity, whereas the biphasic lobes remained. bR thus retained its trimeric conformation with a slight structural deformation. The decreased molar ellipticity resulted from a decoupling of the retinals of adjacent bR when the distance between each retinal increased. This observation indicates a loose structure of delipidated bR with the trimeric configuration and is consistent with the absorption and fluorescence spectra.

3.4. Temporal behavior of intermediate I probed at 460 nm in the presence of surfactants

An ultrafast pump–probe technique was employed to monitor the temporal evolution of the absorption of intermediate I upon excitation with a short pulse. The temporal profiles probed at 460 nm upon excitation of bR at 570 nm are plotted in Figure 4 in the presence of (A) CTAB, (B) SDS and (C) C6E2. The transient population of intermediate I is insignificantly altered within our experimental error upon gradual addition of ionic surfactants CATB and SDS, and neutral surfactant C6E2, as shown in Figure 4. The instrumental response function (bandwidth 200 fs) and a single exponential function were used to fit the experimental data. The experimental and fitted data are plotted on a logarithmic scale in the inset of each frame of Figure 4 over the interval 0.3–1.2 ps. The slope of the fitted line represents the coefficient of the rate of the decay of intermediate I. The satisfactory agreement of the fitted and observed data reveals that a single exponential decay is acceptable to interpret the kinetic behaviors of intermediate I. A lifetime 0.46 ps for intermediate I of the native bR is obtained, in agreement with preceding reports [25]. The ratios of the lifetimes of the surfactant-treated bR relative to native bR are summarized in Figure 5. As the concentrations of the cationic surfactant CTAB and anionic SDS were gradually increased to 0.22 and 1.22 mM, resulting in molar ratios [surfactant]/[bR] = 10.5 and 58.1, respectively the lifetime of intermediate I was observed to increase up to 20%, but an insignificant alteration (within 3%) was observed upon addition of the neutral surfactant C6E2 at concentrations up to 20 mM ([C6E2]/[bR] = 952). The transient population of intermediate J that follows intermediate I is not heavily perturbed upon the treatment with surfactants under our experimental conditions (see Supplementary materials).

Previous experiments on mutagenesis [24], chemical perturbation [25] and physical treatment [23] have been performed to address the interactive conformational alteration that produces a

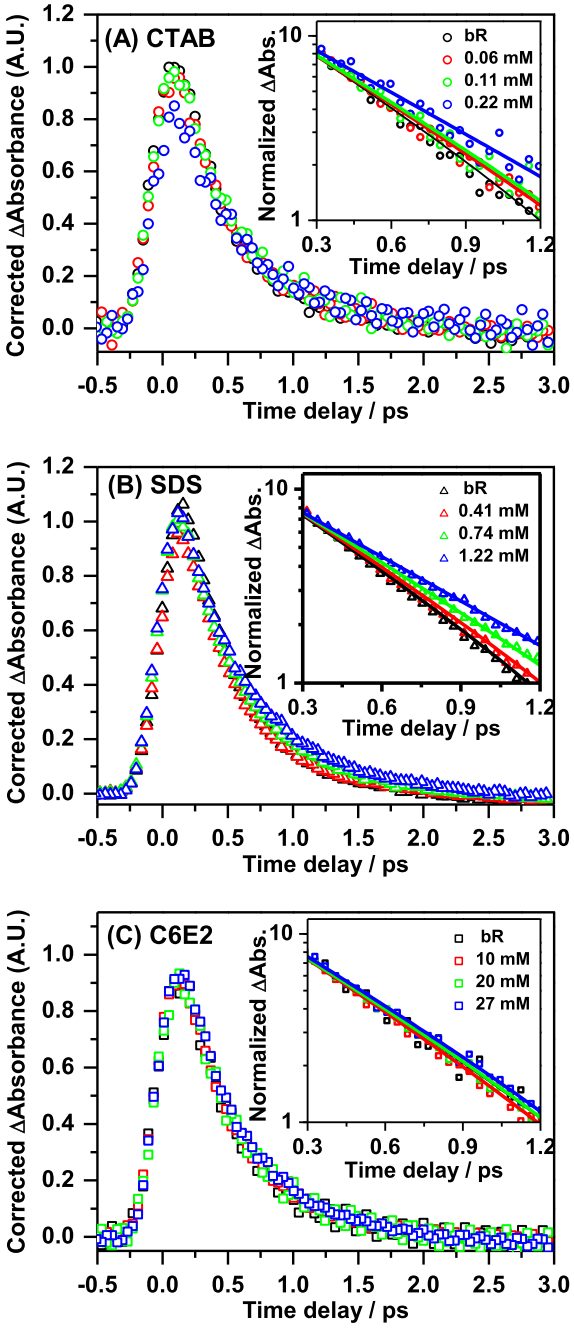

Figure 4. Temporal profiles of the absorbance of intermediate I at 460 nm in the presence of (A) CTAB, (B) SDS and (C) C6E2 at varied concentrations. The corrected Δ*A* is normalized with respect to the absorbance at 568 nm in the steady-state spectra. The insets show a semilogarithmic plot of the normalized absorbance as a function of time from 0.3 to 1.2 ps. The dots and solid lines represent the experimental and fitted data, respectively. The concentrations of the bR and buffer solution are 21 μM and 1.25 mM, respectively.

charge redistribution around the retinal, which is responsible for the altered potential-energy surface for the retinal isomerization. Upon the addition of Triton X-100, the lifetime of intermediate I of the monomeric bR increases about 25% relative to the trimeric ones [25]. The monomerized bR is responsible for a charge redistribution and a dipole reorientation within the retinal-binding cavity. The substitution of the charged amino acids around the retinal vicinity with neutral ones also prolonged the lifetime of intermediate I [24]. Our observed increase by ~20% in lifetime indicates that a surfactant-induced conformational alteration affects the vicinity

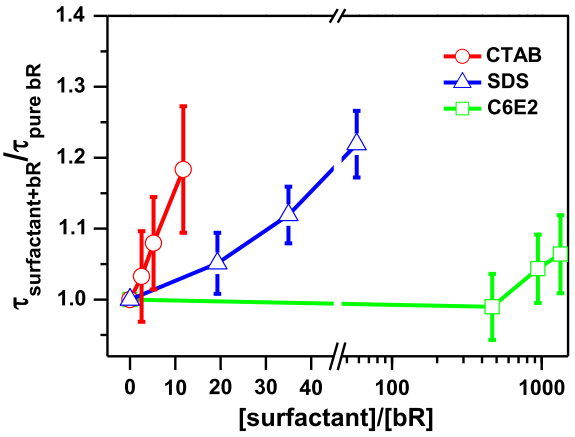

Figure 5. Ratios of the lifetimes of intermediate I of the surfactant-treated bR relative to the native bR at varied [surfactant]/[bR]. Increasing the concentrations of the surfactants slows the decay. The concentrations of bR and buffer solution are maintained at 21 μM and 1.25 mM, respectively.

of the protonated Schiff base, resulting in modified photoisomerization kinetics. Several theoretical predictions also serve to explain our observations.

Multiconfigurational second-order perturbation theory was employed to predict the photoisomerization pathway of the protonated Schiff base with varied chain lengths in the isolated condition (i.e., *in vacuo*) [41,42]. The chemical environment and the charge distribution in the retinal cavity were shown to be strongly correlated with the dynamics of the excited state. Cembran et al. demonstrated that the location of the negative charges of the acetate group of the amino acids adjacent to the retinal can serve as a suitable tool to tune the rate of isomerization at the level CASPT2//CASSCF [16]. When the negative charge distribution is in the middle of the C_{13}=C_{14} bond, a barrierless isomerization path for S_1 is predicted. In contrast, when the negative charge is located near the Schiff base or in the vicinity of the carbon tail, a barrier is expected. The observed decrease in the rate of decay of intermediate I upon treatment with the ionic surfactants is presumably due to the surfactant-induced conformational change and the alteration of the reaction coordinate of the retinal isomerization in terms of the electrostatic interaction of the retinal and the adjacent amino acids. The surfactant-induced partial delipidation of bR exhibits a loose structure, which results in a weak interaction between the retinal and the adjacent amino acids. Away from the equilibrium condition in the native bR, the barrier for retinal isomerization increases; the rate of isomerization of intermediate I consequently decreases. The hypochromic retinal absorption of surfactant-treated bR also indicates that the bond length of the interior retinal is altered. If an alternation of the average bond length, defined as the average of the bond lengths of single bonds minus that of double bonds, is increased, the corresponding absorption contour exhibits a blue shift [43]. As a result, an altered geometry affects the potential-energy surface and is responsible for the varied dynamics.

4. Conclusions

We investigated the kinetics of the reactive excited-state of bacteriorhodopsin upon surfactant treatment with an ultrafast pump–probe transient absorption technique and observed that the ionic surfactants prolonged the lifetime of intermediate I more effectively than the neutral surfactant. The steady-state absorption and CD spectra indicated that the surfactant-treated bR retained its trimeric configuration, but was partially delipidated. Upon excitation at 280 nm, a bathochromic fluorescence near 350 nm supports that the delipidated trimeric bR is exposed to a more aqueous environment. Because lipids were removed, a structural alteration is expected and is proposed to be responsible for the prolonged lifetime of intermediate I. The redistribution of charge around the retinal vicinity might increase the barrier for the all-*trans* to 13-*cis* isomerization around the C_{13}=C_{14} bond. Our observations provide evidence that a surfactant-induced delipidated bR exhibits an altered structure that is responsible for the varied kinetics of the reactive excited state.

Acknowledgments

National Science Council of Taiwan (NSC 99-2113-M-007-019-MY2, NSC 99-2745-M-009-001-ASP) provided support for this research. Bacteriorhodopsin cells were grown from master slants of *Halobacterium halobium* S-9 strain, kindly provided by Professor M. A. El-Sayed at Georgia Institute of Technology. We thank Professor Jia-Cherng Horng and Ming-Chou Lu at National Tsing Hua University for assisting with CD measurements.

Appendix A. Supplementary data

Supplementary data associated with this article can be found, in the online version, at http://dx.doi.org/10.1016/j.cplett.2012.05.006.

References

[1] N.V. Katre, P.K. Wolber, W. Stoeckenius, R.M. Stroud, Proc. Natl. Acad. Sci. USA 78 (1981) 4068.
[2] D. Oesterhelt, W. Stoeckenius, Nat. New Biol. 233 (1971) 149.
[3] J.K. Lanyi, G. Váró, Isr. J. Chem. 35 (1995) 365.
[4] J. Dobler, W. Zinth, W. Kaiser, D. Oesterhelt, Chem. Phys. Lett. 144 (1988) 215.
[5] R.A. Mathies, C.H. Brito Cruz, W.T. Pollard, C.V. Shank, Science 240 (1988) 777.
[6] B. Schmidt, C. Sobotta, B. Heinz, S. Laimgruber, M. Braun, P. Gilch, Biochim. Biophys. Acta 1706 (2005) 165.
[7] K.C. Hasson, F. Gai, P.A. Anfinrud, Proc. Natl. Acad. Sci. USA 93 (1996) 15124.
[8] F. Gai, K.C. Hasson, J.C. McDonald, P.A. Anfinrud, Science 279 (1998) 1886.
[9] Q. Zhong, S. Ruhman, M. Ottolenghi, M. Sheves, N. Friedman, G.H. Atkinson, J.K. Delaney, J. Am. Chem. Soc. 118 (1996) 12828.
[10] S. Ruhman, B. Hou, N. Friedman, M. Ottolenghi, M. Sheves, J. Am. Chem. Soc. 124 (2002) 8854.
[11] T. Kobayashi, T. Saito, H. Ohtani, Nature 414 (2001) 531.
[12] S. Shim, J. Dasgupta, R.A. Mathies, J. Am. Chem. Soc. 131 (2009) 7592.
[13] L. Song, M.A. El-Sayed, J. Am. Chem. Soc. 120 (1998) 8889.
[14] R. Diller, in: M. Braun, P. Gilch, W. Zinth (Eds.), Ultrashort Laser Pulses in Biology and Medicine, Springer-Verlag, 2008, p. 243.
[15] S. Hayashi, E. Tajkhorshid, K. Schulten, Biophys. J. 85 (2003) 1440.
[16] A. Cembran, F. Bernardi, M. Olivucci, M. Garavelli, J. Am. Chem. Soc. 126 (2004) 16018.
[17] H. Abramczyk, J. Chem. Phys. 120 (2004) 11120.
[18] H. Tachikawa, T. Iyama, J. Photochem. Photobiol. B 76 (2004) 55.
[19] A. Warshel, Z.T. Chu, J. Phys. Chem. B 105 (2001) 9857.
[20] P. Altoè, A. Cembran, M. Olivucci, M. Garavelli, Proc. Natl. Acad. Sci. USA 107 (2010) 20172.
[21] S.L. Logunov, L. Song, M.A. El-Sayed, J. Phys. Chem. 98 (1994) 10674.
[22] G. Zgrablić, K. Voïtchovsky, M. Kindermann, S. Haacke, M. Chergui, Biophys. J. 88 (2005) 2779.
[23] A. Biesso, W. Qian, M.A. El-Sayed, J. Am. Chem. Soc. 130 (2008) 3258.
[24] L. Song, M.A. El-Sayed, J.K. Lanyi, Science 261 (1993) 891.
[25] J. Wang, S. Link, C.D. Heyes, M.A. El-Sayed, Biophys. J. 83 (2002) 1557.
[26] L.-K. Chu, M.A. El-Sayed, Photochem. Photobiol. 86 (2010) 316.
[27] L.-K. Chu, M.A. El-Sayed, Photochem. Photobiol. 86 (2010) 70.
[28] D. Oesterhelt, W. Stoeckenius, Methods Enzymol. 31 (1974) 667.
[29] M. Rehorek, M.P. Heyn, Biochemistry 18 (1979) 4977.
[30] C.-W. Chang, C.K. Chou, I-J. Chang, Y.-P. Lee, E.W.-G. Diau, J. Phys. Chem. C 111 (2007) 13288.
[31] B. Becher, F. Tokunaga, T.G. Ebrey, Biochemistry 17 (1978) 2293.
[32] I. Szundi, W. Stoeckenius, Proc. Natl. Acad. Sci. USA 84 (1987) 3681.
[33] V. Kumar, V.K. Sharma, D.S. Kalonia, Int. J. Pharm. 294 (2005) 193.
[34] H.G. Khorana, G.E. Gerber, W.C. Herlihy, C.P. Gray, R.J. Anderegg, K. Nihei, K. Biemann, Proc. Natl. Acad. Sci. USA 76 (1979) 5046.
[35] R.A. Bogomolni, L. Stubbs, J.K. Lanyi, Biochemistry 17 (1978) 1037.
[36] Y.K. Reshetnyak, Y. Koshevnik, E.A. Burstein, Biophys. J. 81 (2001) 1735.
[37] S. Schenkl, F. van Mourik, G. van der Zwan, S. Haacke, M. Chergui, Science 309 (2005) 917.
[38] B.J. Plotkin, W.V. Sherman, Biochemistry 23 (1984) 5353.

[39] M.P. Heyn, P.-J. Bauer, N.A. Dencher, Biochem. Biophys. Res. Comm. 67 (1975) 897.
[40] J.Y. Cassim, Biophys. J. 63 (1992) 1432.
[41] R. González-Luque, M. Garavelli, F. Bernardi, M. Merchán, M.A. Robb, M. Olivucci, Proc. Natl. Acad. Sci. USA 97 (2000) 9379.
[42] L. De Vico, C.S. Page, M. Garavelli, F. Bernardi, R. Basosi, M. Olivucci, J. Am. Chem. Soc. 124 (2002) 4124.
[43] S. Sekharan, K. Morokuma, J. Am. Chem. Soc. 133 (2011) 4734.